Journal of Applied Physics

Effects of B and In on the band structure of BGa(In)As alloys

Cite as: J. Appl. Phys. **132**, 193104 (2022); https://doi.org/10.1063/5.0125109
Submitted: 09 September 2022 • Accepted: 30 October 2022 • Published Online: 17 November 2022

Qian Meng, Rasha H. El-Jaroudi, R. Corey White, et al.

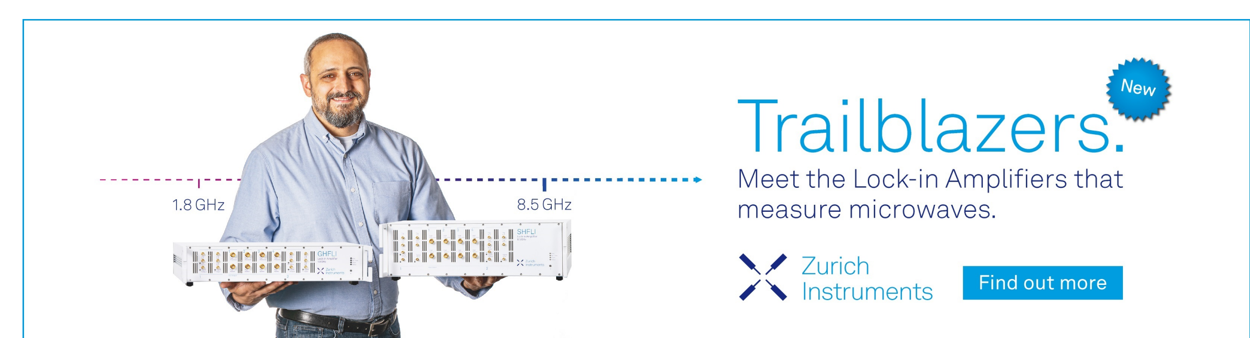

© 2022 Author(s).

Journal of Applied Physics ARTICLE scitation.org/journal/jap

Effects of B and In on the band structure of BGa(In)As alloys

Cite as: J. Appl. Phys. **132**, 193104 (2022); doi: 10.1063/5.0125109
Submitted: 9 September 2022 · Accepted: 30 October 2022 ·
Published Online: 17 November 2022

View Online

Export Citation

CrossMark

Qian Meng,[1] Rasha H. El-Jaroudi,[1] R. Corey White,[1] Tuhin Dey,[2] M. Shamim Reza,[2] Seth R. Bank,[1] and Mark A. Wistey[2,3,a)]

AFFILIATIONS

[1]Microelectronics Research Center and ECE Department, The University of Texas at Austin, Austin, Texas 78758, USA
[2]Materials Science, Engineering, and Commercialization Program, Texas State University, San Marcos, Texas 78666, USA
[3]Physics Department, Texas State University, San Marcos, Texas 78666, USA

[a)]**Author to whom correspondence should be addressed:** mwistey@txstate.edu

ABSTRACT

Highly mismatched semiconductor alloys (HMAs) offer unusual combinations of bandgap and lattice constant, which are attractive for myriad applications. Dilute borides, such as BGa(In)As, are typically assumed to be HMAs. BGa(In)As can be grown in higher alloy compositions than Ga(In)NAs with comparable bandgaps, potentially enabling routes to lattice-matched telecom lasers on Si or GaAs. However, BGa(In)As remains relatively unexplored, especially with large fractions of indium. Density functional theory with HSE06 hybrid functionals was employed to study BGaInAs with 4%–44% In and 0%–11% B, including atomic rearrangement effects. All compositions showed a direct bandgap, and the character of the lowest conduction band was nearly unperturbed with the addition of B. Surprisingly, although the bandgap remained almost constant and the lattice constant followed Vegard's law with the addition of boron, the electron effective mass increased. The increase in electron effective mass was higher than in conventional alloys, though smaller than those characteristics of HMAs. This illustrates a particularly striking finding, specifically that the compositional space of BGa(In)As appears to span conventional alloy and HMA behavior, so it is not well-described by either limit. For example, adding B to GaAs introduces additional states within the conduction band, but further addition of In removes them, regardless of the atomic arrangement.

Published under an exclusive license by AIP Publishing. https://doi.org/10.1063/5.0125109

I. INTRODUCTION

Highly mismatched semiconductor alloys (HMAs) have been intensely investigated for several decades due to their ability to adjust lattice constant and/or bandgap with a dilute amount of mismatched atom incorporation. This offers tremendous new freedom for designers of photonic and electronic devices by offering a much broader range of functional materials that can be grown lattice-matched on common substrates such as GaAs or Si.[1,2] For example, adding small amounts of N to GaAs or InGaAs can sharply reduce both bandgap and lattice constant at the same time.[3–7] However, the incorporation of nitrogen into conventional III–V alloys is limited by its low solid solubility and challenging growth.[8–12]

Unlike the large electronegativity difference between Group V elements As and N ($\Delta X = 0.86$ eV) in dilute nitrides, the difference in electronegativity between Group III elements Ga and B is much smaller, 0.23 eV, although the size mismatch is comparable with that of As–N. Additionally, the theoretical solid solubility of B is much larger than N,[8] which potentially makes it easier to grow B–III–V alloys compared with N–III–V alloys. Indeed, we recently demonstrated up to 22% B substitutional incorporation in BGaAs by molecular beam epitaxy (MBE) while maintaining excellent crystallinity.[13–17] These results strongly suggest that B could offer a much wider range of strain engineering compared with N–III–V alloys.

Previous experimental studies of BGaAs were generally limited to B concentrations lower than 10% due to challenging crystal growth.[18–24] Simultaneous incorporation of In and B to grow BGaInAs is even more difficult due to the increased growth variables. Similarly, previous investigations of BGaInAs were limited to a combination of low In (<10%) concentration and higher B (~4%) concentration, or else higher In (~40%) but low B (~2%) concentration.[25–27] With our recent improvements in crystal growth, there is a strong motivation for a more complete theoretical

understanding of BGa(In)As alloys for devices. Both the electronic and optical properties of BGaInAs remain unknown over a wide range of B and In concentrations that would be necessary for lattice-matched integration on GaAs or Si, particularly at telecom wavelengths. We have previously reported that around 3.5% B and 44% In is needed for a quantum well on GaAs emitting at wavelengths near 1.3 μm.[14,17,28] Better modeling would help target longer wavelengths near 1.55 μm.

In dilute nitrides such as GaInNAs, the addition of N strongly perturbs the conduction band, splitting the band edge.[29] The perturbation introduced by boron in BGaAs is predicted to be much weaker, and a conventional, GaAs-like conduction band edge can even be restored by adding indium.[30,31] Our previous work also showed that adding In to BGaAs increases the photoluminescence (PL) intensity about three times,[28] which generally agrees with previous reports of adding B to InGaAs multiple quantum wells (MQWs).[26] However, the mechanism leading to the increased PL, whether intrinsic to the material or dependent on growth conditions, was unknown. Additionally, in the dilute nitrides, the lattice position of the highly mismatched atom relative to its Group III nearest neighbors influences the material properties such as strain energy, bandgap, and the strength of optical transitions.[32,33] Conversely, in the dilute boride arsenides, such as BGa(In)As, all of the variations is on the Group III sublattice: B–As–Ga, B–As–In, B–As–B, etc. The effects of such ordering are poorly understood; HMAs such as BGaInAs are notoriously poor candidates for approximate techniques such as the virtual crystal approximation, making simulation more challenging. Also, B–B split interstitials and other defects at high B concentrations can also exist in BGa(In)As, although such defects are beyond the scope of this paper.

In this work, we used density functional theory (DFT) with hybrid functionals to study the evolution of the band structure as B and In are added to GaAs. B concentrations in the Group III lattice were 0%, 3.7%, 7.4%, and 11.1%, and In concentrations were 0%, 3.7%, and 44%. The effects of local bonding configurations such as B–As–In vs B–As–B were also compared to study the effects of annealing and random alloys. We find that BGaInAs closely resembles a conventional III–V alloy, in contrast to other HMAs such as dilute nitrides. These results predict BGa(In)As to be a highly promising material for near-IR optoelectronics on Si and GaAs, with a direct bandgap and sharp conduction band (CB) edge.

II. METHODS

The Vienna *Ab initio* Simulation Package (VASP), based on DFT[34] using the projector-augmented wave (PAW) method,[35] was used to model 54 atom supercells of BGaInAs. HSE06 hybrid functionals were used, as these have been shown to provide more accurate bandgaps with reasonable computational efficiency,[36,37] and for comparison with the other published work.[38] Plane waves with energy up to 478 eV were included in the basis set for DFT.[39] The convergence criterion between electronic steps was $\Delta E < 10^{-8}$ eV for all supercells studied here. The Brillouin zone was sampled using a $3 \times 3 \times 3$ Γ-centered, Monkhorst–Pack grid. The supercells were constructed using a $3 \times 3 \times 3$ repetition of the two-atom zinc-blende primitive unit cell along the primitive lattice vectors. In all configurations discussed below, each B or In atom replaced a Ga atom. To obtain the band structure of BGaInAs, the atomic structure of BGa(In)As was first optimized by fully relaxing the ion positions for a series of different lattice constants, then fitting the Birch–Murnaghan equation to obtain the lattice constant producing the lowest system energy, and finally re-relaxing the supercell at that new lattice constant before extracting optical properties and band structures. The use of supercells leads to folding of band structure, which complicates the direct comparison of different configurations, so BandUP was used to unfold or project the band structure into the first Brillouin zone.[40–43] Additionally, spin–orbital coupling (SOC) would slightly decrease the bandgap and break the degeneracy of the split-off valence band. SOC was not included here due to its severe computational cost. Without SOC, the energies and effective masses near the valence band maximum

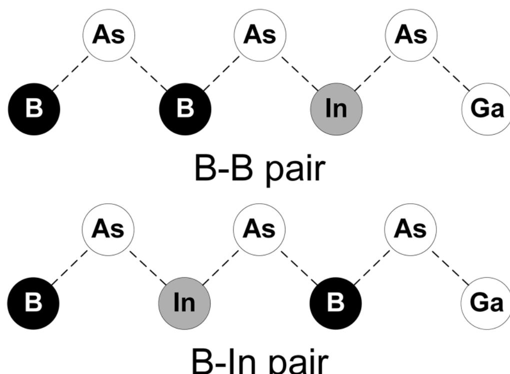

FIG. 1. Schematic of atom bonding for B–B pair (B–As–B bonds) and B–In pair (B–As–In bonds).

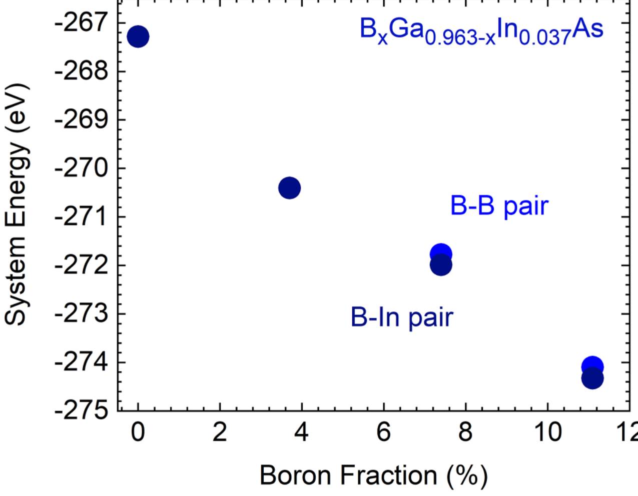

FIG. 2. Ground state system energy for B–B pair and B–In pair configurations for various fractions of B in $B_xGa_{0.963-x}In_{0.037}As$.

Published under an exclusive license by AIP Publishing

TABLE I. Supercell construction for B–In pair configuration.

Configuration for B–In pair			
	0% In	3.7% In	44% In
3.7% B	$B_1Ga_{26}As_{27}$	$B_1Ga_{25}In_1As_{27}$	$B_1Ga_{14}In_{12}As_{27}$
7.4% B	$B_2Ga_{25}As_{27}$	$B_2Ga_{24}In_1As_{27}$	$B_2Ga_{13}In_{12}As_{27}$
11.1% B	$B_3Ga_{24}As_{27}$	$B_3Ga_{23}In_1As_{27}$	$B_3Ga_{12}In_{12}As_{27}$

are incorrect, but the conduction band is still expected to be qualitatively correct, particularly when comparing relative changes.[39]

III. RESULTS AND DISCUSSION

A. Validation using binaries

The resulting lattice constant of fully relaxed BGaInAs closely followed Vegard's law, showing a highly linear relation between element concentration and lattice constant for atoms perfectly in the substitutional position. To validate the model, lattice constants of binary GaAs, InAs, and BAs were calculated to be 5.6674, 6.1083, and 4.7711 Å respectively, in good agreement with experimental values of 5.6532, 6.0583, and 4.777 Å, respectively.[44] Similarly, GaAs had a computational (experimental) bandgap of 1.354 eV (1.424 eV). The calculated InAs bandgap was 0.379 eV, which is slightly above the experiment bandgap (0.354 eV) but consistent with the range predicted by other hybrid functional HSE calculation reports[37,45–48] since we did not impose any quasi-empirical adjustments such as artificial strain. Our calculation of BAs showed a direct bandgap of 4.12 eV and an indirect bandgap of 2.02 eV at the CB minimum (CBM) near X, which agrees well with a recent experimental study of BAs[49] and other BAs calculation results using hybrid functionals.[50,51] Nevertheless, to reduce the effects of possible errors in bandgaps compared with the experiment, this work focused on relative changes in the band structure due to composition. Therefore, the same computational parameters were used to calculate the optical properties of BGaInAs.

B. Atom arrangements

In highly mismatched alloy systems, different local arrangements of the highly mismatched atoms strongly influence the material properties.[32,33] This paper follows the notation of cluster configuration suggested by Bellaiche and Zunger.[32] Two B atom bonding configurations were constructed as shown in Fig. 1: (1) B–B pairs, where the B atoms are directly connected to the same As atom forming B–As–B bonds and (2) B–In pairs, where the In atom is the first Group III nearest neighbor of B, forming B-As-In bonds. As

TABLE II. Supercell construction for B–B pair configuration.

Configuration for B–B pair		
	3.7% In	44% In
7.4% B	$B_2Ga_{24}In_1As_{27}$	$B_2Ga_{13}In_{12}As_{27}$
11.1% B	$B_3Ga_{23}In_1As_{27}$	$B_3Ga_{12}In_{12}As_{27}$

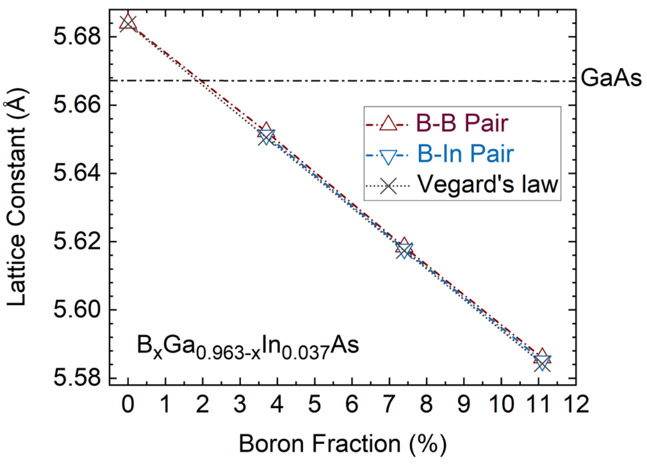

FIG. 3. Lattice constant in $B_xGa_{0.963-x}In_{0.037}As$ for B–B pair and B–In pair configuration when adding B compared with lattice constant calculated using Vegard's law. GaAs dash-dotted line is calculated from VASP. Lines are a guide to the eye.

shown in Fig. 2, B–B pairs and B–In pairs have approximately equal system energy, indicating that the two configurations are equally likely to form. Therefore, we must study both configurations to investigate the properties when adding B to InGaAs. For each bonding configuration, three In concentrations (0%, 3.7%, and 44%) were used, and the B concentration varied from 0% to 11.1%. This allowed us to study the effects of the addition of B and In to BGa

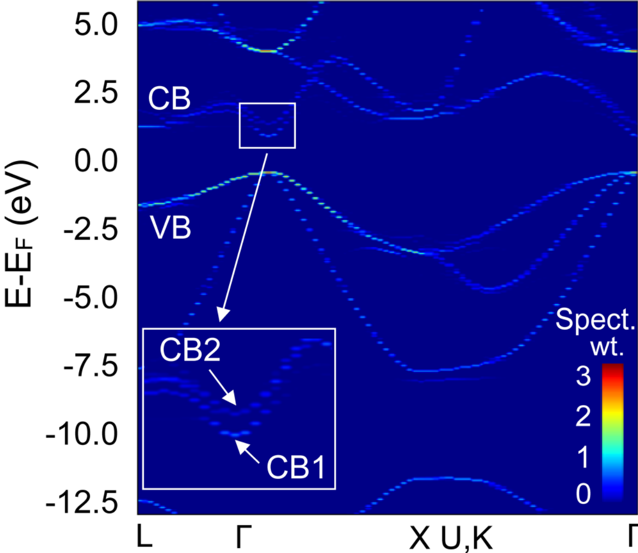

FIG. 4. Unfolded band structure of $B_{0.037}Ga_{0.963}As$. Inset: Magnified view of conduction band splitting at Γ. High spectral weight means a state is similar to one or more equivalent states in the GaAs primitive unit cell.

Published under an exclusive license by AIP Publishing

(In)As individually. Configurations constructed based on 54-atom supercells used in this work are summarized Tables I and II.

C. Structural properties

While deviations from Vegard's law have been previously predicted in dilute B alloys with both positive and negative bowing parameters,[52,53] Fig. 3 shows a relationship between boron concentration and lattice constant that is as linear as other III–V alloys.

D. Electronic properties

In all compositions of B and In calculated in this work, BGaInAs remained a direct bandgap material. Unfolded band structures of BGa(In)As with B–In pair atom arrangement are shown in Figs. 4 and 5. The unfolded band structure of BGaAs at a low B concentration of 3.7% is shown in Fig. 4. The CBM was distinctly split into two bands in $B_{0.037}Ga_{0.963}As$, labeled CB1 and CB2. The conduction band splitting is also observed in low-In $B_{0.037}Ga_{0.926}In_{0.037}As$ with B–In pairs, as shown in Fig. 5(c). However, the band splitting vanishes with a further increase in In concentration. As shown in Fig. 5(d), there was only one high spectral weight state near the CBM at the Γ point. Additionally, for higher B fractions (7.4%, 11.1%) with 0% and 3.7% In, several extra CB states appear in Figs. 5(f) and 5(g), which agree well with the extra cluster states near the CBM observed in Lindsey's calculations.[30,31] At low In concentrations in $B_xGa_{0.963-x}In_{0.037}As$, the total number of CB states increases when the B concentration is increased. We attribute these additional states to the influences brought by a short range interaction of B atoms. A detailed study of the properties of the extra states near conduction band minimum will be reported elsewhere. In contrast, the number of CB states decreased when adding more indium. In contrast, in high-indium $B_xGa_{0.56-x}In_{0.44}As$, the number of CB states near the bandgap remains at 2 even with 11.1% B, indicating that adding In makes BGaInAs more like a traditional III–V alloy.

Despite the increasing number of CB states with increasing B concentration at low In concentration, the conduction band minimum, i.e., the lowest conduction band state at zone center, retains a large spectral weight, showing it resembles the CB of unperturbed GaAs.[42,43] Figure 6 shows the spectral weight of CB states when adding B and In in both B–In pair and B–B pair configurations. The lowest conduction band of BGa(In)As in all compositions has a spectral weight ranging from 0.6 to 0.9, while the spectral weight for higher CB states is smaller than 0.4. Therefore, the lowest CB state (CB1) in BGa(In)As is much less perturbed by B than higher CB states are.

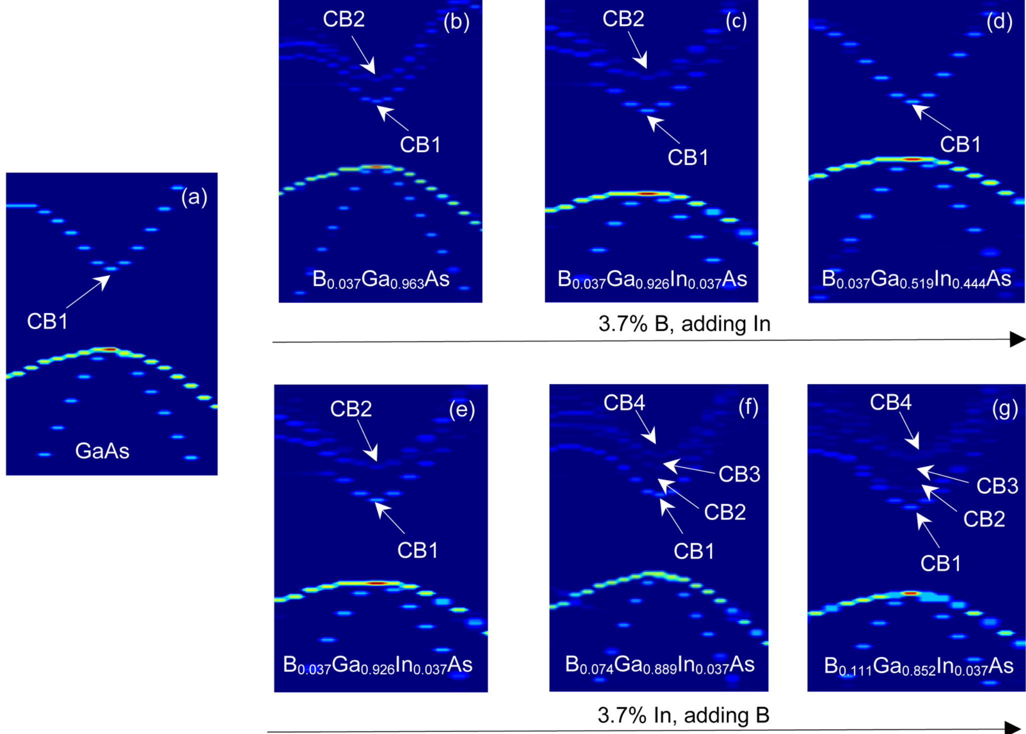

FIG. 5. Evolution of CB states with B and In for the B–In pair configuration near zone center. White arrows highlight states at zone center: (a) Pristine GaAs with only one state at zone center, (b) $B_{0.037}Ga_{0.963}As$ with band splitting, (c) $B_{0.037}Ga_{0.926}In_{0.037}As$ with band splitting at low In concentration, (d) $B_{0.037}Ga_{0.519}In_{0.444}$ with restored conduction band similar to pristine GaAs, (e) $B_{0.037}Ga_{0.926}In_{0.037}As$ with band splitting, (f) $B_{0.074}Ga_{0.889}In_{0.037}As$ with four conduction band states, and (g) $B_{0.111}Ga_{0.852}In_{0.037}As$ with four conduction band states at high B concentration.

Published under an exclusive license by AIP Publishing

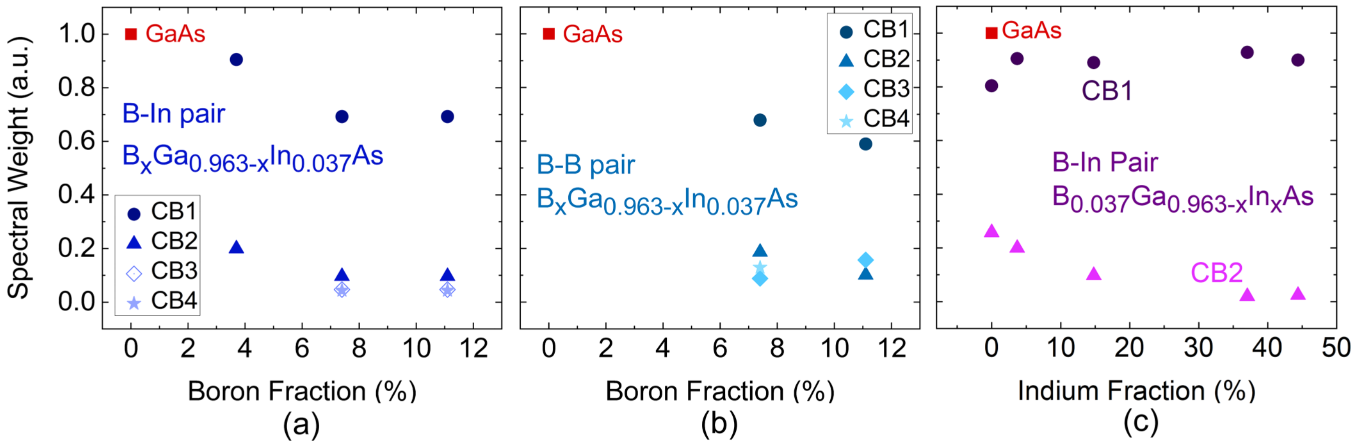

FIG. 6. Spectral weight (SW) of states at conduction band (CB) near zone center in (a) B–In pair $B_xGa_{0.963-x}In_{0.037}As$, with x from 0.037 to 0.111, (b) B–B pair $B_xGa_{0.963-x}In_{0.037}As$, $x = 0.074–0.111$, and (c) B–In pair $B_{0.037}Ga_{0.963-x}In_xAs$, $x = 0–0.444$.

In contrast, all compositions showed almost no effect of B on the valence band maximum (VBM), in agreement with reports from Lindsay and O'Reilly.[30] The projections onto atomic orbitals of all CB states further suggest that the lowest CB state at the Γ point is optically active, like the GaAs CBM, supported by calculations of the optical matrix element, which will be reported elsewhere. As shown in Fig. 7, the s orbital portion of CB1 only slightly decreases when adding B compared with the 100% s-like GaAs CBM, while adding In increases the s orbital composition of the CB1. The high spectral weight and small change in s orbital composition of CB1 show a relatively unperturbed conduction band minimum. These results indicate adding B to GaAs has a relatively small influence on the direct gap transition from the VBM to the CBM at zone center ($k = 0$). In some ways, it appears that adding In to BGaAs removes the perturbation induced by adding B. Detailed investigations of optical properties and transitions in BGaInAs are under way and will be reported elsewhere.

Previous experimental and theoretical studies of dilute B alloys reported a sharp increase in electron effective mass when adding B.[30,54] This is often attributed to band anticrossing of the CB with an isoelectronic impurity state that is nearly flat in k-space, leading to a flatter CB edge. The effective mass was calculated from the band structure over a k-space length of approximately 0.02 $Born^{-1}$. First, we calculated the electron effective mass of GaAs to be $m_e^* = 0.067$ times the electron rest mass m_0, in good agreement with the experiment.[55] The calculation results for a constant In concentration of 3.7% in BGaInAs suggest that adding

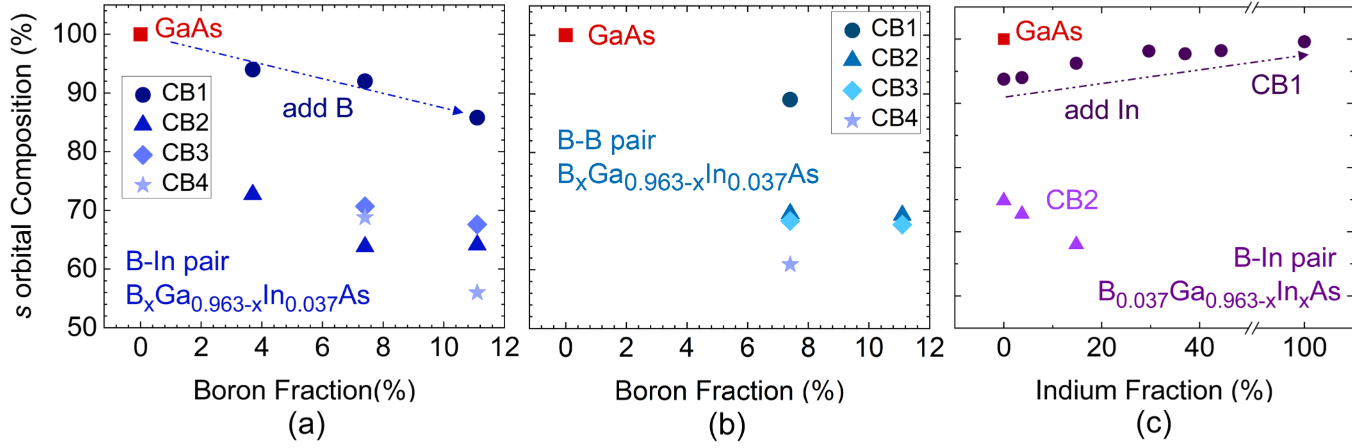

FIG. 7. s orbital composition of CB states near zone center: (a) for B–In pair $B_xGa_{0.963-x}In_{0.037}As$, $x = 0.037–0.111$; (b) for B–B pair $B_xGa_{0.963-x}In_{0.037}As$, $x = 0.074–0.111$; and (c) for B–In pair $B_{0.037}Ga_{0.963-x}In_xAs$, $x = 0–0.444$.

Published under an exclusive license by AIP Publishing

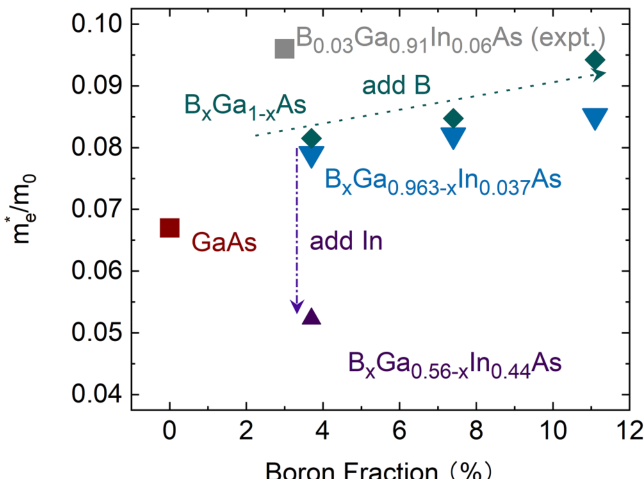

FIG. 8. Electron effective mass for B–In pair $B_xGa_{0.963-x}In_{0.037}As$ when adding B. The experimental electron effective mass was measured using far-infrared magneto-optic generalized ellipsometry studies in Ref. 54.

B increases the electron effective mass, as shown in Fig. 8. However, the increased electron effective mass when adding B is still much smaller than the hole effective mass. On the other hand, adding In sharply decreases the electron effective mass, just as it does in conventional InGaAs. Overall, the increase in m_e* is much smaller for dilute borides than dilute nitrides,[56,57] which again shows BGa(In)As behaves more like a traditional III–V alloy.

Together, these results show that adding B to GaAs only has small influences on the band structure near $k = 0$ compared with other HMAs such as dilute nitrides. The bandgap remains direct, the energies of the CBM are only slightly perturbed, and the CBM and VBM retain their respective *s*-like and *p*-like character. Likewise, the electron effective mass only slightly increases when adding B. Adding In further removes the band splitting introduced by B. We believe the similarity with conventional III–V alloys can be explained by the small difference in electronegativity between B and the atom it replaces, i.e., Ga. In other words, BGaAs qualifies as a highly mismatched alloy only in atomic size differences, but not in electronegativity. We believe BGaInAs, therefore, offers greater potential for adjusting lattice constant to lattice-match to GaAs and Si without the severe mismatch effects induced by other highly mismatched alloys.

IV. CONCLUSIONS

This work explored the band structure and electronic properties of BGa(In)As with B concentration ranging from 0% to 11% and In concentration ranging from 0% to 44% using DFT with HSE06 hybrid functionals. We found that the properties of BGa(In)As are in between conventional III–V alloys and HMAs, which we attribute to the relatively small difference in electronegativity when B replaces Ga. The fully relaxed lattice parameter of BGa(In)As was found to closely follow Vegard's law. The lowest CB state in BGa(In)As strongly resembles the lowest unperturbed GaAs CB, as shown by a high spectral weight after band unfolding and similar wavefunction compared with GaAs. The CB splits into two or more states with the addition of just 3.7% B, and only the lowest band retains GaAs-like character. On the other hand, this splitting disappears with increasing In concentration, with a direct bandgap and roughly obeying the virtual crystal approximation for bandgap and optical properties regardless of atom arrangement. In addition, adding B slightly increases the electron effective mass more than the virtual crystal approximation would predict, but less than might be expected from band anticrossing in other HMAs. In any case, the perturbation of the conduction band minimum and electron effective mass is relatively small compared with other HMAs, and the conduction band minimum remains direct and optically active across the entire range of B and In concentrations studied. Thus, BGaInAs is a highly promising material for lattice-matched lasers and other near-infrared optoelectronics on Si and GaAs.

ACKNOWLEDGMENTS

This work was also supported by the National Science Foundation (NSF) (Award Nos. ECCS-1933836, DMR-1508646, and CBET-1438608). The authors also acknowledge the Learning, Exploration, Analysis, and Processing (LEAP) cluster at Texas State University for computing resources. This work was performed in part at the University of Texas Microelectronics Research Center, a member of the National Nanotechnology Coordinated Infrastructure (NNCI), which is supported by the NSF (No. ECCS-1542159).

AUTHOR DECLARATIONS

Conflict of Interest

The authors have no conflicts to disclose.

Author Contributions

Qian Meng: Conceptualization (equal); Data curation (equal); Formal analysis (equal); Investigation (equal); Methodology (equal); Software (equal); Validation (equal); Writing – original draft (equal); Writing – review & editing (equal). **Rasha H. El-Jaroudi:** Conceptualization (equal); Data curation (equal); Formal analysis (equal); Investigation (equal); Writing – review & editing (equal). **R. Corey White:** Formal analysis (supporting); Writing – review & editing (supporting). **Tuhin Dey:** Methodology (supporting); Software (supporting). **M. Shamim Reza:** Software (supporting). **Seth R. Bank:** Conceptualization (equal); Data curation (equal); Formal analysis (equal); Funding acquisition (equal); Investigation (equal); Methodology (equal); Resources (equal); Supervision (equal); Validation (equal); Writing – review & editing (equal). **Mark A. Wistey:** Conceptualization (equal); Data curation (equal); Formal analysis (equal); Funding acquisition (equal); Investigation (equal); Methodology (equal); Resources (equal); Software (equal); Supervision (equal); Validation (equal); Writing – review & editing (equal).

Published under an exclusive license by AIP Publishing

DATA AVAILABILITY

The data that support the findings of this study are available from the corresponding author upon reasonable request.

REFERENCES

[1]D. B. Jackrel, S. R. Bank, H. B. Yuen, M. A. Wistey, Jr., J. S. Harris, A. J. Ptak, and S. R. Kurtz, "Dilute nitride GaInNAs and GaInNAsSb solar cells by molecular beam epitaxy," J. Appl. Phys. **101**(11), 114916 (2007).

[2]C. A. Stephenson, W. A. O'Brien, M. W. Penninger, W. F. Schneider, M. Gillett-Kunnath, J. Zajicek, and M. A. Wistey, "Band structure of germanium carbides for direct bandgap silicon photonics," J. Appl. Phys. **120**(5), 053102 (2016). doi:

[3]M. Kondow, K. Uomi, K. Hosomi, and T. Mozume, "Gas-source molecular beam epitaxy of GaN_xAs_{1-x} using a N radical as the N source," Jpn. J. Appl. Phys. **33**(8A), L1056 (1994).

[4]M. Weyers, M. Sato, and H. Ando, "Red shift of photoluminescence and absorption in dilute GaAsN alloy layers," Jpn. J. Appl. Phys. **31**(7A), L853 (1992).

[5]K. Uesugi, N. Morooka, and I. Suemune, "Reexamination of N composition dependence of coherently grown GaNAs band gap energy with high-resolution x-ray diffraction mapping measurements," Appl. Phys. Lett. **74**(9), 1254–1256 (1999).

[6]T. Makimoto, H. Saito, T. Nishida, and N. Kobayashi, "Excitonic luminescence and absorption in dilute $GaAs_{1-x}$ N x alloy (x< 0.3%)," Appl. Phys. Lett. **70**(22), 2984–2986 (1997).

[7]M. Sato, "Growth of GaAsN by low-pressure metalorganic chemical vapor deposition using plasma-cracked N_2," J. Cryst. Growth **145**(1–4), 99–103 (1994).

[8]G. L. Hart and A. Zunger, "Electronic structure of BAs and boride III-V alloys," Phys. Rev. B **62**(20), 13522 (2000).

[9]K. Osamura, S. Naka, and Y. Murakami, "Preparation and optical properties of $Ga_{1-x}In_xN$ thin films," J. Appl. Phys. **46**(8), 3432–3437 (1975).

[10]R. Goldman, R. Feenstra, B. Briner, M. O'steen, and R. Hauenstein, "Atomic-scale structure and electronic properties of GaN/GaAs superlattices," Appl. Phys. Lett. **69**(24), 3698–3700 (1996).

[11]R. Kuroiwa, H. Asahi, K. Asami, S.-J. Kim, K. Iwata, and S. Gonda, "Optical properties of GaN-rich side of GaNP and GaNAs alloys grown by gas-source molecular beam epitaxy," Appl. Phys. Lett. **73**(18), 2630–2632 (1998).

[12]M. Takahashi, A. Moto, S. Tanaka, T. Tanabe, S. Takagishi, K. Karatani, M. Nakayama, K. Matsuda, and T. Saiki, "Observation of compositional fluctuations in GaNAs alloys grown by metalorganic vapor-phase epitaxy," J. Crystal Growth **221**(1–4), 461–466 (2000).

[13]K. M. McNicholas, R. H. El-Jaroudi, H. Maczko, G. Cossio, L. J. Nordin, S. D. Sifferman, R. Kudrawiec, E. T. Yu, D. Wasserman, and S. R. Bank, "BGaAs/GaP heteroepitaxy for strain-free luminescent layers on Si," in *60th Electronic Material Conference, Santa Barbara, CA, USA* (Materials Research Society, 2018).

[14]R. H. El-Jaroudi, K. M. McNicholas, A. F. Briggs, S. D. Sifferman, L. Nordin, and S. R. Bank, "Room-temperature photoluminescence and electroluminescence of 1.3-μm-range BGaInAs quantum wells on GaAs substrates," Appl. Phys. Lett. **117**, 021102 (2020).

[15]K. M. McNicholas, R. H. El-Jaroudi, and S. R. Bank, "Kinetically limited molecular beam epitaxy of $B_xGa_{1-x}As$ alloys," J. Cryst. Growth Des. **21**(12), 6076–6082 (2021).

[16]J. Kopaczek, F. Dybala, S. J. Zelewski, N. Sokolowski, W. Zuraw, K. M. McNicholas, R. H. El-Jaroudi, R. C. White, S. R. Bank, and R. Kudrawiec, "Photoreflectance studies of temperature and hydrostatic pressure dependencies of direct optical transitions in BGaAs alloys grown on GaP," J. Phys. D: Appl. Phys. **55**(1), 015107 (2021).

[17]R. H. El-Jaroudi, K. M. McNicholas, H. S. Maczko, R. Kudrawiec, and S. R. Bank, "Growth advancement of GaAs-based BGaInAs alloys emitting at 1.3 μm by molecular beam epitaxy," J. Crys. Growth Des. **22**(6), 3753–3759 (2022).

[18]J. F. Geisz, D. J. Friedman, J. M. Olson, S. R. Kurtz, R. C. Reedy, A. B. Swartzlander, B. M. Keyes, and A. G. Norman, "BGaInAs alloys lattice-matched to GaAs," Appl. Phys. Lett. **76**(11), 1443–1445 (2000).

[19]V. Gupta, M. Koch, N. Watkins, Y. Gao, and G. Wicks, "Molecular beam epitaxial growth of BGaAs ternary compounds," J. Electron. Mater. **29**(12), 1387–1391 (2000).

[20]W. Shan, W. Walukiewicz, J. Wu, K. M. Yu, J. W. Ager III, S. X. Li, E. E. Haller, J. F. Geisz, D. J. Friedman, and S. R. Kurtz, "Band-gap bowing effects in $BxGa_{1-x}As$ alloys," J. Appl. Phys. **93**(5), 2696–2699 (2003).

[21]V. Gottschalch, G. Leibiger, and G. Benndorf, "MOVPE growth of $B_xGa_{1-x}As$, $B_xGa_{1-x-y}In_yAs$, and $B_xAl_{1-x}As$ alloys on (0 0 1) GaAs," J. Cryst. Growth **248**, 468–473 (2003).

[22]R. Hamila, F. Saidi, A. Fouzri, L. Auvray, Y. Monteil, and H. Maaref, "Clustering effects in optical properties of BGaAs/GaAs epilayers," J. Lumin. **129**(9), 1010–1014 (2009).

[23]S. Ilahi, F. Saidi, R. Hamila, N. Yacoubi, H. Maaref, and L. Auvray, "Shift of the gap energy and thermal conductivity in BGaAs/GaAs alloys," Phys. B **421**, 105–109 (2013).

[24]S. Ku, "Preparation and properties of boron arsenides and boron arsenide-gallium arsenide mixed crystals," J. Electrochem. Soc. **113**(8), 813 (1966).

[25]R. Hamila, F. Saidi, P. H. Rodriguez, L. Auvray, Y. Monteil, and H. Maaref, "Growth temperature effects on boron incorporation and optical properties of BGaAs/GaAs grown by MOCVD," J. Alloys Compd. **506**(1), 10–13 (2010).

[26]Q. Wang, Z. Jia, X. Ren, Y. Yan, Z. Bian, X. Zhang, S. Cai, and Y. Huang, "Effect of boron incorporation on the structural and photoluminescence properties of highly-strained $In_xGa_{1-x}As$/GaAs multiple quantum wells," AIP Adv. **3**, 072111 (2013).

[27]J. F. Geisz, D. J. Friedman, and S. Kurtz, in *Proceedings of the 20th IEEE Photovoltaic Specialists Conference* (IEEE, 2000).

[28]R. H. El-Jaroudi, K. M. McNicholas, B. A. Bouslog, I. E. Olivares, R. C. White, J. A. McArthur, and S. R. Bank, "Boron alloys for GaAs-based 1.3 μm semiconductor lasers," in *2019 Conference on Lasers and Electro-Optics (CLEO)* (IEEE, 2019), pp. 1–2.

[29]W. Shan, W. Walukiewicz, J. W. Ager III, E. E. Haller, J. F. Geisz, D. J. Friedman, J. M. Olson, and S. R. Kurtz, "Band anticrossing in GaInNAs alloys," Phys. Rev. Lett. **82**(6), 1221 (1999).

[30]A. Lindsay and E. O'Reilly, "Theory of conduction band dispersion in dilute $B_xGa_{1-x}As$ alloys," Phys. Rev. B **76**(7), 075210 (2007).

[31]A. Lindsay and E. P. O'Reilly, "Theory of electronic structure of BGaAs and related alloys," Phys. Status Solidi **5**, 454–459 (2008).

[32]L. Bellaiche and A. Zunger, "Effects of atomic short-range order on the electronic and optical properties of GaAsN, GaInN, and GaInAs alloys," Phys. Rev. B **57**(8), 4425 (1998).

[33]P. Kent and A. Zunger, "Evolution of III-V nitride alloy electronic structure: The localized to delocalized transition," Phys. Rev. Lett. **86**(12), 2613 (2001).

[34]G. Kresse and J. Furthmüller, "Efficient iterative schemes for *ab initio* total-energy calculations using a plane-wave basis set," Phys. Rev. B **54**(16), 11169 (1996).

[35]P. E. Blöchl, "Projector augmented-wave method," Phys. Rev. B **50**(24), 17953 (1994).

[36]J. Heyd, G. E. Scuseria, and M. Ernzerhof, "Hybrid functionals based on a screened Coulomb potential," J. Chem. Phys. **118**(18), 8207–8215 (2003).

[37]J. Heyd, J. E. Peralta, G. E. Scuseria, and R. L. Martin, "Energy band gaps and lattice parameters evaluated with the Heyd-Scuseria-Ernzerhof screened hybrid functional," J. Chem. Phys. **123**(17), 174101 (2005).

[38]C. Freysoldt, and J. Neugebauer, "Point defects in supercells: Correction schemes for the dilute limit," in *ICMR Workshop on Ab-Initio Description of Charged Systems and Solid/Liquid Interfaces* (ICMR, 2014).

[39]I. Gulyas, R. Kudrawiec, and M. A. Wistey, "Electronic structure of $B_xGa_{1-x}As$ alloys using hybrid functionals," J. Appl. Phys. **126**(9), 095703 (2019).

[40]T. B. Boykin, N. Kharche, G. Klimeck, and M. Korkusinski, "Approximate bandstructures of semiconductor alloys from tight-binding supercell calculations," J. Phys.: Condens. Matter **19**(3), 036203 (2007).

Published under an exclusive license by AIP Publishing

[41]V. Popescu and A. Zunger, “Extracting E vs k → Effective band structure from supercell calculations on alloys and impurities,” Phys. Rev. B **85**(8), 085201 (2012).
[42]P. V. Medeiros, S. Stafström, and J. Björk, “Effects of extrinsic and intrinsic perturbations on the electronic structure of graphene: Retaining an effective primitive cell band structure by band unfolding,” Phys. Rev. B **89**(4), 041407 (2014).
[43]P. V. Medeiros, S. S. Tsirkin, S. Stafström, and J. Björk, “Unfolding spinor wave functions and expectation values of general operators: Introducing the unfolding-density operator,” Phys. Rev. B **91**(4), 041116 (2015).
[44]I. Vurgaftman, J. R. Meyer, and L. R. Ram-Mohan, “Band parameters for III–V compound semiconductors and their alloys,” J. Appl. Phys. **89**(11), 5815–5875 (2001).
[45]J. Paier, M. Marsman, K. Hummer, G. Kresse, I. C. Gerber, and J. G. Ángyán, “Screened hybrid density functionals applied to solids,” J. Chem. Phys. **124**(15), 154709 (2006).
[46]T. Shimazaki and Y. Asai, “Energy band structure calculations based on screened Hartree–Fock exchange method: Si, AlP, AlAs, GaP, and GaAs,” J. Chem. Phys. **132**(22), 224105 (2010).
[47]F. Tran and P. Blaha, “Accurate band gaps of semiconductors and insulators with a semilocal exchange-correlation potential,” Phys. Rev. Lett. **102**(22), 226401 (2009).
[48]H.-P. Komsa and A. Pasquarello, “Dangling bond charge transition levels in AlAs, GaAs, and InAs,” Appl. Phys. Lett. **97**(19), 191901 (2010).
[49]B. Song, K. Chen, K. Bushick, K. A. Mengle, F. Tian, G. A. G. U. Gamage, Z. Ren, E. Kioupakis, and G. Chen, “Optical properties of cubic boron arsenide,” Appl. Phys. Lett. **116**(14), 141903 (2020).
[50]J. Buckeridge and D. O. Scanlon, “Electronic band structure and optical properties of boron arsenide,” Phys. Rev. Mater. **3**(5), 051601 (2019).
[51]I. Bravić and B. Monserrat, “Finite temperature optoelectronic properties of BAs from first principles,” Phys. Rev. Mater. **3**(6), 065402 (2019).
[52]N. Chimot, J. Even, H. Folliot, and S. Loualiche, “Structural and electronic properties of BAs and $B_xGa_{1-x}As$, $B_xIn_{1-x}As$ alloys,” Phys. B **364**(1–4), 263–272 (2005).
[53]S. Murphy, A. Chroneos, C. Jiang, U. Schwingenschlögl, and R. Grimes, “Deviations from Vegard’s law in ternary III-V alloys,” Phys. Rev. B **82**(7), 073201 (2010).
[54]T. Hofmann, M. Schubert, G. Leibiger, and V. Gottschalch, “Electron effective mass and phonon modes in GaAs incorporating boron and indium,” Appl. Phys. Lett. **90**(18), 182110 (2007).
[55]W. Nakwaski, “Effective masses of electrons and heavy holes in GaAs, InAs, AlAs and their ternary compounds,” Phys. B **210**(1), 1–25 (1995).
[56]P. Hai, W. Chen, I. Buyanova, H. Xin, and C. Tu, “Direct determination of electron effective mass in GaNAs/GaAs quantum wells,” Appl. Phys. Lett. **77**(12), 1843–1845 (2000).
[57]Z. Pan, L. Li, Y. Lin, B. Sun, D. Jiang, and W. Ge, “Conduction band offset and electron effective mass in GaInNAs/GaAs quantum-well structures with low nitrogen concentration,” Appl. Phys. Lett. **78**(15), 2217–2219 (2001).

Published under an exclusive license by AIP Publishing